nature geoscience

LETTERS

PUBLISHED ONLINE: 22 FEBRUARY 2009 | DOI: 10.1038/NGEO443

Human amplification of drought-induced biomass burning in Indonesia since 1960

Robert D. Field[1]*, Guido R. van der Werf[2] and Samuel S. P. Shen[3]

Much of the interannual variability in global atmospheric carbon dioxide concentrations has been attributed to variability of emissions from biomass burning[1–3]. Under drought conditions, burning in Indonesia is a disproportionate contributor to these emissions, as seen in the 1997/98 haze disaster[1,4]. Yet our understanding of the frequency, severity and underlying causes of severe biomass burning in Indonesia is limited because of the absence of satellite data that are useful for fire monitoring before the mid-1990s. Here we present a continuous monthly record of severe burning events from 1960 to 2006 using the visibility reported at airports in the region. We find that these fires cause extremely poor air quality conditions and that they occur only during years when precipitation falls below a well defined threshold. Historically, large fire events have occurred in Sumatra at least since the 1960s. By contrast, the first large fires are recorded in Kalimantan (Indonesian Borneo) in the 1980s, despite earlier severe droughts. We attribute this difference to different patterns of changes in land use and population density. Fires in Indonesia have often been linked with El Niño[1,2,5–12], but we find that the Indian Ocean Dipole pattern is as important a contributing factor.

The Indonesian haze disaster in 1997/98 (refs 1,4) had pronounced regional impacts on air quality[9]. Average emissions from the region are smaller than those from Africa, but are comparable to emissions from the Amazon basin[4]. As most emissions in Indonesia stem from peat fires and deforestation, with limited forest regrowth, they contribute to the build-up of CO_2 in the atmosphere. Future fire risk in Indonesia will be sensitive to potentially drier conditions[13] and increases in anthropogenic landscape disturbance[14–16].

During 1997–2006, there were two major fire episodes in Indonesia (1997/98, 2006) and two minor episodes (2002, 2004) detected in the Global Fire Emissions Database (GFED; ref. 4), which occurred during droughts of different strengths[12,15]. Before this, there are no high-quality, continuous records of the fires. There are, however, case-by-case accounts of coincident drought and fire years during the 1980s and early 1990s in Indonesia[6], also detected in elevated ozone and aerosol concentrations from the Total Ozone Mapping Spectrometer[5,17], and predominantly linked to El Niño-induced droughts. Fires are observed almost year-round, but the main fire season starts as early as July and lasts until mid-November, typically peaking in September and October.

The Indonesian fires are unique in that the bulk of emissions is due to the continuous burning of peat soils for up to four consecutive months[1], which produces aerosol concentrations high enough to significantly reduce visibility[7,10]. To better understand the severity of biomass burning haze and its underlying causes, we used visibility records from Sumatra and Kalimantan's World Meteorological Organization level meteorological stations to calculate monthly mean extinction coefficients (B_{ext}). Regional mean B_{ext} was computed for Sumatra and Kalimantan, each of which had three stations with data back to 1960 (Fig. 1). We computed B_{ext} using the Koschmeider relationship, omitting observations where present weather codes indicated precipitation or fog (see Supplementary Section S1).

We found an excellent correspondence between regional B_{ext} and TPM estimates from the GFED for both Sumatra ($R^2 = 91$, Fig. 2a,b) and Kalimantan ($R^2 = 0.85$, Fig. 3a,b) for the period of 1997–2006. We note that the two data sources are entirely independent, with the GFED data being derived largely from remote-sensing data and biogeochemical modelling[4], and the B_{ext} being derived from simple meteorological observations at airports. As an indication of the severity of the 1997 haze event and its impact on air quality, the extreme monthly B_{ext} values from stations near the centre of the main burning regions (maximum 16.6 km^{-1}, high values indicating poor visibility) were over five times greater than the extreme monthly B_{ext} values at the cities recognized as having the world's worst air quality (maximum 3.1 km^{-1}) (see Supplementary Table S1).

In Sumatra, the extended B_{ext} data captured events in 1991 and 1994, and to a lesser degree that of 1982 (Fig. 2b). These events were coincident with elevated ozone concentrations detected by the Total Ozone Mapping Spectrometer sensor[5]. There were also large events in 1961, 1963 and 1972 of a slightly lesser magnitude than those in the 1990s, but easily distinguishable from the background B_{ext} level. All events from 1960 to 2006 occurred during periods of anomalously low seasonal rainfall (Fig. 2c).

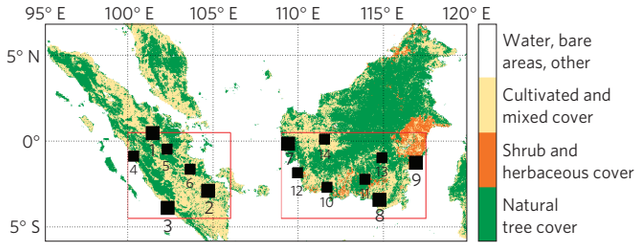

Figure 1 | Land cover from Global Land Cover 2000 (ref. 29) and World Meteorological Organization stations used in the analysis, listed in Supplementary Table S1. Stations 1–3 and 7–9 were used in the long-term analysis. The red boxes outline the regions over which total particulate matter (TPM) emissions, precipitation and population were analysed for Sumatra (0.5° N–4.5° S, 100° E–106° E) and Kalimantan (0.5° N–4.5° S, 109° E–117.5° E).

[1]Department of Physics, University of Toronto, Toronto, M5S 1A7, Canada, [2]Faculty of Earth and Life Sciences, VU University Amsterdam, Amsterdam, 1081HV, Netherlands, [3]Department of Mathematics and Statistics, San Diego State University, San Diego 92182, USA. *e-mail: robert.field@utoronto.ca.

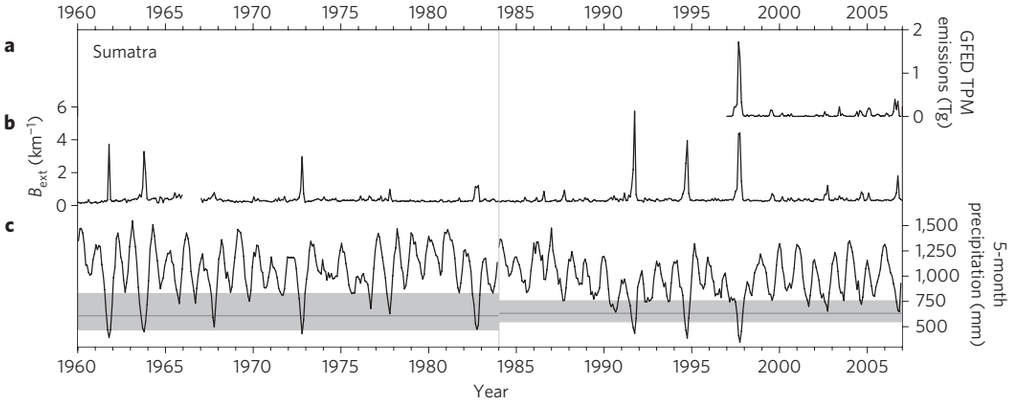

Figure 2 | Monthly time-series for Sumatra. a, GFED TPM emission estimates[4], **b**, mean B_{ext}, and **c**, five-month back-totalled precipitation from the NCEP Precipitation over Land (PRECL) data[27] for 1960–1983 and the Global Precipitation Climatology Project[28] for 1984–2006. The grey vertical line separates the two analysis periods. The grey horizontal lines in **c** show the estimated precipitation threshold α during each period, and the shading shows the 95% confidence interval for α. Supplementary Fig. S1 shows the B_{ext} and precipitation data in a scatter-plot view. See the Methods section for a description of the precipitation data and threshold definition.

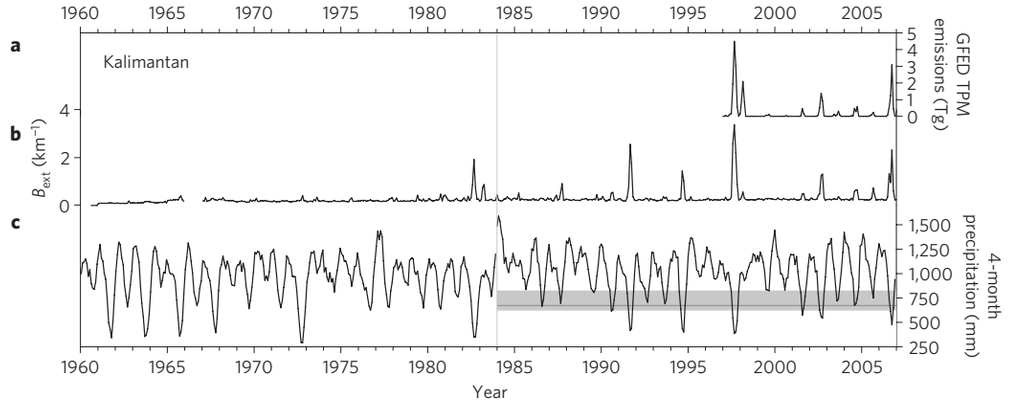

Figure 3 | Monthly time-series for Kalimantan. a, GFED TPM emission estimates[4], **b**, mean B_{ext}, and **c**, four-month back-totalled PRECL precipitation for 1960–1983 and Global Precipitation Climatology Project precipitation for 1984–2006. The grey vertical line separates the two analysis periods. The grey horizontal line in **c** shows the estimated precipitation threshold α during 1984–2006, and the shading shows the 95% confidence interval for α. No threshold is shown for 1960–1983, owing to the poor fit of the model. Supplementary Fig. S2 shows the B_{ext} and precipitation data in a scatter-plot view. See the Methods section for a description of the precipitation data and threshold definition.

Conversely, severe events were absent during non-drought years, despite regular dry seasons.

We estimated the nonlinear relationship between precipitation and haze using piecewise linear regression, splitting the data into an early period (1960–1983) and recent period (1984–2006) to detect any possible changes in the sensitivity of fire to drought. The piecewise model includes a threshold parameter α, which separates normal precipitation conditions from those under which severe haze is possible (see the Methods section). We considered back-totalled precipitation of between 2 and 6 months as predictor variables, selecting the back-totalling period that yielded the highest coefficient of determination R^2 as optimal.

In Sumatra during 1960–1983, five-month back-totalled precipitation was the best predictor, explaining 67% of the variance in B_{ext} over Sumatra, with a threshold of 609 mm (see Supplementary Table S2, Fig. 2c). Below this threshold, there was a sensitivity of $-0.011\,km^{-1}\,mm^{-1}$, indicating an increase in B_{ext} with decreasing precipitation (see Supplementary Fig. S1a). During the 1984–2006 period, five-month precipitation could explain 85% of the variance in B_{ext}, with a threshold of 631 mm and a below-threshold sensitivity of $-0.015\,km^{-1}\,mm^{-1}$ (see Supplementary Fig. S1b). The improved predictability during the 1984–2006 period can be attributed in part to the higher-quality precipitation data during that period (see the Methods section), and perhaps to a slightly stronger sensitivity of the Sumatran fire environment to drought.

In Kalimantan, there was a very different history of biomass burning. Severe haze events under drought conditions are evident from 1982 onwards, but unlike those in Sumatra were largely absent during the 1960s and 1970s (Fig. 3b). Atmospheric trajectory analysis showed that the absence of haze during this period was not attributable to differences in wind flow (see Supplementary Section S2). The 1972 and 1997 droughts, for example, had similar patterns of atmospheric transport between the burning region and the visibility stations, but severe haze was observed only in 1997 (see Supplementary Section S2). There is anecdotal evidence of the 1972 haze event being present over Borneo[11], but the absence of the event in the B_{ext} record indicates that it was of a much smaller magnitude than subsequent events, consistent with the absence of fire in East Kalimantan in 1972 (ref. 8).

More quantitatively, the four-month precipitation was the best predictor during 1984–2006 over Kalimantan, explaining 78% of the variance in B_{ext}, with a precipitation threshold of 672 mm and a below-threshold sensitivity of $-0.007\,km^{-1}\,mm^{-1}$

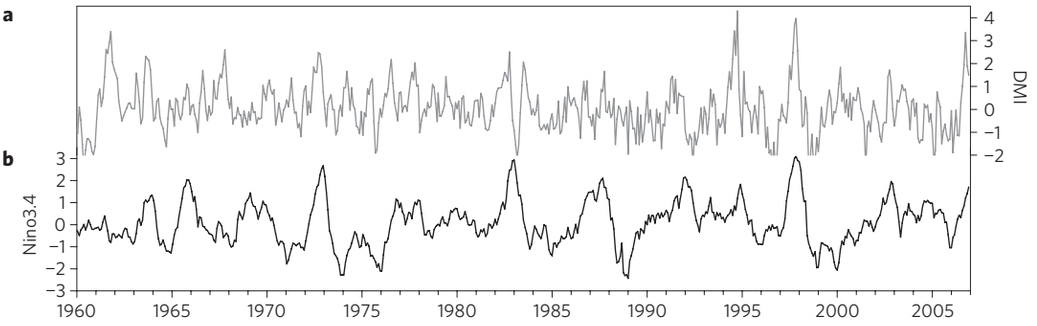

Figure 4 | SST time series. a, Dipole mode index (DMI; ref. 19) and **b**, Nino3.4 index calculated from the Smith and Reynolds global gridded SST analysis[30]. The Nino3.4 index is defined as the standardized SST anomaly over the 5° S–5° N and 170° W–120° W region of the Pacific Ocean. The DMI is defined as the difference of the SST anomalies between the western equatorial Indian Ocean (50° E–70° E, 10° S–10° N) and the southeastern equatorial Indian Ocean (90° E–110° E, 10° S–0° N).

(see Supplementary Table S2, Fig. 3, Supplementary Fig. S2a). In contrast, such a relationship was absent from 1960–1983, with only 13% of the variance in B_{ext} explained by the four-month precipitation, and a below-threshold sensitivity of $-0.001\,km^{-1}\,mm^{-1}$, which was not statistically distinguishable from zero (see Supplementary Fig. S2b). Whereas in Sumatra there was only a small increase in fire sensitivity to drought, the Kalimantan fire environment changed from highly fire resistant to highly fire prone at some point between the droughts of 1972 and 1982.

Drought acts as the trigger for fire occurrence, but it is humans who ignite the fires. How do we explain the difference in the evolution of the fire environments in Sumatra and Kalimantan since the 1960s?

In Indonesia, fire is used primarily to clear vegetation waste, and is closely associated with deforestation and agricultural expansion[6,8,11]. The number of ignitions depends on the extent of these activities, which also tend to lower the resilience of tropical forests to drought through changes in moisture balance[8]. Indonesia's overall annual deforestation rate from 1950 to 1997 was 1.1%, but from 1950 to 1985 the deforestation rate in Kalimantan (0.7%) was half that of Sumatra (1.4%). It was only during 1985 to 1997 that the deforestation rate in Kalimantan (2.2%) began to approach that of Sumatra (2.6%) (see Supplementary Section S3).

Kalimantan's later deforestation is characteristic of broader development patterns, reflected by trends in population and agriculture. Sumatra had population densities more than three times greater than Kalimantan during the first half of the twentieth century (see Supplementary Fig. S3). During the 1960s and 1970s, population growth in Sumatra accelerated rapidly, but lagged behind in Kalimantan, approaching Sumatra's 1960s growth rates only in the 1980s. This difference in population growth between the two regions was in part due to the Indonesian government's policy of transmigration to ease population pressure on Java and, later, to develop Indonesia's remote forested regions. Sumatra was the main target region of transmigration through the 1960s and 1970s, whereas Kalimantan became a significant target region only in the 1980s (see Supplementary Section S4). In Kalimantan, the effects of this population shift on land-cover change were exacerbated by a change in focus from small-scale subsistence agriculture to large-scale industrial agriculture and agro-forestry, which have larger land-use footprints. Peatlands drained under the Mega Rice Project of the 1990s, for example, were the single biggest contributor to emissions across all of Indonesia during the 1997 fire event (see Supplementary Section S3).

Overall, we attribute the difference in evolution of Sumatra's and Kalimantan's fire environments to different patterns of human activity and government policy. Fire has been used for millennia in Indonesia[18], but in the past at a much smaller scale[11]. Much of Kalimantan remained relatively undeveloped until the 1980s, which explains the previous absence of major fire events in the B_{ext} record, despite several severe droughts in the 1960s and 1970s.

In addition to their different development patterns, precipitation over Sumatra and Kalimantan is influenced by different patterns of zonal circulation in the tropics. Whereas haze events have been attributed predominantly to El Niño conditions, there is strong evidence that the Indian Ocean Dipole (IOD) also contributes independently to drought over Indonesia[19,20], and was linked to the 1997 fire event[17,21]. Physically, a combination of local and remote forcings contribute to reduced precipitation over Indonesia. Anomalously cool sea surface temperatures (SSTs) in surrounding seas suppress local convection, but, in combination with warm SST anomalies in the western Indian and eastern Pacific Oceans, also reduce moisture convergence over Indonesia[22,23]. Under El Niño or IOD conditions, this effect strengthens into September[20], as moisture over western Indonesia is transported westward to the Indian Ocean[23].

We examined the influence of the El Niño–Southern Oscillation (ENSO) and IOD specifically over the main burning regions in Fig. 1, comparing the regional precipitation variance explained by the Nino3.4 index and DMI as indicators of ENSO and IOD strength, respectively (Fig. 4). Linear correlations were computed during the July–November period when most burning occurs, and over the entire NCEP PRECL data period of 1948–2006. Over Sumatra, the Nino3.4 SST index could explain 30% of the variability in mean July–November precipitation under a linear model, compared with 61% explained by the DMI. A simple index consisting of the sum of the DMI and the Nino3.4 also explained 61% of the variability in Sumatra precipitation, yielding no improvement over the DMI alone. Over Kalimantan, the Nino3.4 could explain 58% of the variability in precipitation, compared with 49% explained by the DMI, but a combined index could explain 72% of the variability. The strength of these controls was somewhat sensitive to the period analysed, definition of season and particular dataset used, but typically either the DMI or combined Nino3.4–DMI index performed better than the Nino3.4 (see Supplementary Section S5).

It is therefore important that SST anomalies over both the Pacific and Indian Oceans be monitored in preventing and mitigating future fire events. Although the 1994 and 2006 events, for example, did occur during moderate El Niño conditions, it was the positive IOD conditions that distinguished them from 2002, when the drought and haze were weaker (Fig. 4). The 1961 event occurred under neutral ENSO and strongly positive IOD conditions, and the severity of the 1997 event seems to be attributable to the combined strength of the El Niño and the IOD.

With the presence of intensive land-use, severe fire years have occurred when seasonal precipitation was below a given threshold, owing to either or both El Niño and positive IOD conditions. Our precipitation threshold estimates can therefore serve as benchmarks

to identify periods of severe haze risk, aiding in the interpretation of seasonal rainfall outlooks for operational fire management.

Such mitigation measures are particularly important under a changing climate, given the possibility of more persistent El Niño-like conditions[24], reduced rainfall over Indonesia's main burning regions[13] and a positive feedback between reduced soil moisture and reduced precipitation in Indonesia[25]. Among countries with humid tropical forests, Indonesia's current deforestation rate of 3.4% per year is second only to that of Brazil[26]. The extent of large-scale oil palm plantations is projected to increase, partly to meet growing demand for biofuels[14]. As droughts are inevitable and may become more severe, Indonesia's future fire regime depends strongly on the extent of these types of human activity.

Methods

For each region, we considered back-totalled rainfall of up to six months as predictor variables. More sophisticated drought indices were not considered, having been shown for 1997–2006 not to provide any advantage over simple rainfall totals[15]. We used the best available precipitation data for each of the 1960–1983 and 1984–2006 analysis periods. The PRECL dataset[27] beginning in 1948 was used for the 1960–1983 period, but was found to have a much more sparse gauge observation network from the 1980s onwards (see Supplementary Fig. S4). For the 1984–2006 period, we therefore used data from the Global Precipitation Climatology Project[28], which blends satellite and rain gauge observations and covers 1979–present.

We used piecewise regression to estimate the nonlinear relationship between precipitation and B_{ext} (ref. 15). This technique provided an explicit estimate of precipitation threshold, and of the sensitivity of B_{ext} to changes in precipitation below this threshold. Physically, the use of a threshold-based model corresponds to moisture ignition thresholds of fuels, particularly in drained peatland[15]. The model consists of two linear segments, constrained to be equal at an unknown threshold α, and is given by

$$B_{ext} = \begin{cases} \beta_0 + \beta_1 x & x \leqslant \alpha \\ \beta_0 + \beta_1 x + \beta_2 (x - \alpha) & x > \alpha \end{cases}$$

where β_0 is the y intercept, β_1 is the slope of the line below α, $\beta_1 + \beta_2$ is the slope of the line above α and x is a given predictor variable, for example, five-month back-totalled precipitation. The below-threshold slope β_1 quantifies the degree to which B_{ext} varies with precipitation. Across the different back-totalling periods, we assessed goodness of fit using R^2, and provide 95% confidence intervals for all estimated parameters using fully paired bootstrapping with 2,000 re-samples. For each of Sumatra and Kalimantan, the back-totalling period yielding the largest R^2 under the piecewise model was selected for interpretation. Scatter-plot versions of Figs 2 and 3 are shown in Supplementary Figs S1,S2, which emphasize the structure of the piecewise model.

Visibility data used in the analysis can be obtained from the US National Climatic Data Center at: http://www.ncdc.noaa.gov/oa/visibility/.

Received 23 October 2008; accepted 27 January 2009; published online 22 February 2009

References

1. Page, S. E. *et al*. The amount of carbon released from peat and forest fires in Indonesia during 1997. *Nature* **420**, 61–65 (2002).
2. van der Werf, G. R. *et al*. Continental-scale partitioning of fire emissions during the 1997 to 2001 El Nino/La Nina period. *Science* **303**, 73–76 (2004).
3. Langenfelds, R. L. *et al*. Interannual growth rate variations of atmospheric CO_2 and its delta C_{13}, H_2, CH_4, and CO between 1992 and 1999 linked to biomass burning. *Glob. Biogeochem. Cycles* **16**, doi:10.1029/2001gb001466 (2002).
4. van der Werf, G. R. *et al*. Interannual variability in global biomass burning emissions from 1997 to 2004. *Atmos. Chem. Phys.* **6**, 3423–3441 (2006).
5. Kita, K., Fujiwara, M. & Kawakami, S. Total ozone increase associated with forest fires over the Indonesian region and its relation to the El Niño-Southern oscillation. *Atmos. Environ.* **34**, 2681–2690 (2000).
6. Bowen, M. R., Bompard, J. M., Anderson, I. P., Guizol, P. & Gouyon, A. in *Forest Fires and Regional Haze in Southeast Asia* (eds Eaton, P. & Radojevic, M.) 41–66 (Nova Science, 2001).
7. Heil, A. & Goldammer, J. G. Smoke-haze pollution: A review of the 1997 episode in Southeast Asia. *Regional Environ. Change* **2**, 24–37 (2001).
8. Siegert, F., Ruecker, G., Hinrichs, A. & Hoffmann, A. A. Increased damage from fires in logged forests during droughts caused by El Nino. *Nature* **414**, 437–440 (2001).
9. Kunii, O. *et al*. The 1997 haze disaster in Indonesia: Its air quality and health effects. *Arch. Environ. Health* **57**, 16–22 (2002).
10. Wang, Y. H., Field, R. D. & Roswintiarti, O. Trends in atmospheric haze induced by peat fires in Sumatra Island, Indonesia and El Nino phenomenon from 1973–2003. *Geophys. Res. Lett.* **31**, doi:10.1029/2003GL018853 (2004).
11. Aiken, S. R. Runaway fires, smoke-haze pollution, and unnatural disasters in Indonesia. *Geogr. Rev.* **94**, 55–79 (2004).
12. Logan, J. A. *et al*. Effects of the 2006 El Nino on tropospheric composition as revealed by data from the Tropospheric Emission Spectrometer (TES). *Geophys. Res. Lett.* **35**, doi:10.1029/2007GL031698 (2008).
13. Li, W. H. *et al*. Future precipitation changes and their implications for tropical peatlands. *Geophys. Res. Lett.* **34**, doi:10.1029/2006GL028364 (2007).
14. Fargione, J., Hill, J., Tilman, D., Polasky, S. & Hawthorne, P. Land clearing and the biofuel carbon debt. *Science* **319**, 1235–1238 (2008).
15. Field, R. D. & Shen, S. S. P. Predictability of carbon emissions from biomass burning in Indonesia from 1997 to 2006. *J. Geophys. Res.* **113**, doi:10.1029/2008jg000694 (2008).
16. van der Werf, G. R. *et al*. Climate regulation of fire emissions and deforestation in equatorial Asia. *Proc. Natl Acad. Sci. USA* **105**, 20350–20355 (2008).
17. Thompson, A. M. *et al*. Tropical tropospheric ozone and biomass burning. *Science* **291**, 2128–2132 (2001).
18. Anshari, G., Kershaw, A. P. & van der Kaars, S. A late Pleistocene and Holocene pollen and charcoal record from peat swamp forest, Lake Sentarum Wildlife Reserve, West Kalimantan, Indonesia. *Paleogeogr. Paleoclimatol. Paleoecol.* **171**, 213–228 (2001).
19. Saji, N. H., Goswami, B. N., Vinayachandran, P. N. & Yamagata, T. A dipole mode in the tropical Indian Ocean. *Nature* **401**, 360–363 (1999).
20. Hong, C. C., Lu, M. M. & Kanamitsu, M. Temporal and spatial characteristics of positive and negative Indian Ocean dipole with and without ENSO. *J. Geophys. Res.* **113**, doi:10.1029/2007JD009151 (2008).
21. Abram, N. J., Gagan, M. K., Mcculloch, M. T., Chappell, J. & Hantoro, W. S. Coral Reef death during the 1997 Indian Ocean dipole linked to Indonesian Wildfires. *Science* **301**, 952–955 (2003).
22. Hendon, H. H. Indonesian rainfall variability: Impacts of ENSO and local air–sea interaction. *J. Clim.* **16**, 1775–1790 (2003).
23. Juneng, L. & Tangang, F. T. Evolution of ENSO-related rainfall anomalies in Southeast Asia region and its relationship with atmosphere-ocean variations in Indo-Pacific sector. *Clim. Dyn.* **25**, 337–350 (2005).
24. Vecchi, G. A. & Soden, B. J. Global warming and the weakening of the tropical circulation. *J. Clim.* **20**, 4316–4340 (2007).
25. Notaro, M. Statistical identification of global hot spots in soil moisture feedbacks among IPCC AR4 models. *J. Geophys. Res.* **113**, doi:10.1029/2007JD009199 (2008).
26. Hansen, M. C. *et al*. Humid tropical forest clearing from 2000 to 2005 quantified by using multitemporal and multiresolution remotely sensed data. *Proc. Natl Acad. Sci. USA* **105**, 9439–9444 (2008).
27. Chen, M. Y., Xie, P. P., Janowiak, J. E. & Arkin, P. A. Global land precipitation: A 50-Yr monthly analysis based on gauge observations. *J. Hydrometeorol.* **3**, 249–266 (2002).
28. Adler, R. F. *et al*. The Version-2 Global Precipitation Climatology Project (GPCP) monthly precipitation analysis (1979-Present). *J. Hydrometeorol.* **4**, 1147–1167 (2003).
29. Stibig, H. J. *et al*. A land-cover map for South and Southeast Asia derived from SPOT-VEGETATION data. *J. Biogeogr.* **34**, 625–637 (2007).
30. Smith, T. M. & Reynolds, R. W. Extended reconstruction of global sea surface temperatures based on COADS data (1854–1997). *J. Clim.* **16**, 1495–1510 (2003).

Acknowledgements

We thank W. Spangler at the National Center for Atmospheric Research for assistance in processing the visibility data, C. Hong for assistance with Supplementary Section S5 and N. MacKendrick, K. Moore and B. de Groot for helpful reviews. R.D.F. was supported by a Natural Sciences and Engineering Research Council of Canada scholarship, and G.R.v.d.W. by a Veni grant from the Netherlands Organization for Scientific Research.

Author contributions

R.D.F. conceived of the study and conducted the data analysis under the graduate supervision of S.S.P.S. All authors contributed to interpretation of the results and writing of the manuscript.

Additional information

Supplementary Information accompanies this paper on www.nature.com/naturegeoscience. Reprints and permissions information is available online at http://npg.nature.com/reprintsandpermissions. Correspondence and requests for materials should be addressed to R.D.F.